Available online at www.sciencedirect.com
SCIENCE DIRECT
Journal of the European Ceramic Society 26 (2006) 2639–2645
www.elsevier.com/locate/jeurceramsoc

Strengthening of ceramics by shot peening

Wulf Pfeiffer*, Tobias Frey

Fraunhofer Institute for Mechanics of Materials (IWM), Wöhlerstr. 11, 79108 Freiburg, Germany

Received 6 April 2005; received in revised form 2 June 2005; accepted 11 June 2005
Available online 18 August 2005

Abstract

Shot peening is a common finishing procedure to improve the static and cyclic strength of metal components. Recent investigations showed that, under specific shot peening conditions, also in brittle ceramics high compressive stresses up to more than 1 GPa can be introduced near the surface which increase the near-surface strength. The presentation compiles the actual potential of the shot peening process for alumina and in detail for silicon nitride ceramics. The influence of shot peening parameters on the residual stress state, dislocation density, topography, static and cyclic and rolling near-surface strength is determined.

Keywords: Al_2O_3; Si_3N_4; Strength; Toughening; Wear resistance; Shot peening

1. Introduction

Shot peening is a common procedure to improve the static and cyclic strength of metal components. It is based on a multiple localized plastic deformation of near-surface regions. This results in a surface layer which is improved by strain-hardening (increase of dislocation density) and macroscopic compressive residual stresses (Fig. 1).

Non-transformation toughened ceramics show the typical brittle material behaviour of failure before deformation at room temperature. Thus, strengthening of ceramics due to deformation induced compressive residual stresses has been thought to be not possible.

Recent investigations show, however[1,2] that, under specific shot peening conditions, also in brittle materials like ceramics high compressive stresses up to more than 1 GPa can be introduced near the surface. Exposing these strengthened surfaces to loading situations, which are characterized by a steep near-surface stress gradient, a boost of load capacity could be obtained. Such loading situations exist in, e.g., roller and sliding bearings or metal forming tools.

The aim of this paper is to compile the present potential of the shot peening process for three different types of ceramics.

2. Experimental details

2.1. Materials investigated

Commercially available alumina and silicon nitride ceramics were investigated. Table 1 summarizes the materials and the most important material characteristics.

2.2. Shot peening

The shot peening tests were carried out with a modified injection system. The pressurized air and the shot are applied to the jet nozzle in two different tubes. The shot is accelerated in the nozzle to a high velocity and hits the specimen's surface. The shot used was tungsten carbide beads with a diameter of 610–690 μm. The peening pressure ranged from 0.2 up to 0.4 MPa. Typical peening times were 280–840 s for flat samples and – due to the larger surface – 22 min for rolling samples. The resulting Almen-intensity was in the range of 0.22–0.28 mmA (the Almen (A)-intensity is determined from the curvature of a strip of the thickness 1.29 mm

* Corresponding author. Tel.: +49 761 5142 166; fax: +49 761 5142 403.
E-mail address: wulf.pfeiffer@iwm.fhg.de (W. Pfeiffer).

0955-2219/$ – see front matter © 2005 Elsevier Ltd. All rights reserved.
doi:10.1016/j.jeurceramsoc.2005.06.036

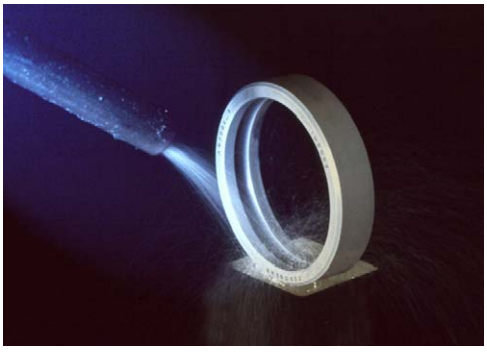

Fig. 1. Shot peening of a ceramic-bearing ring.

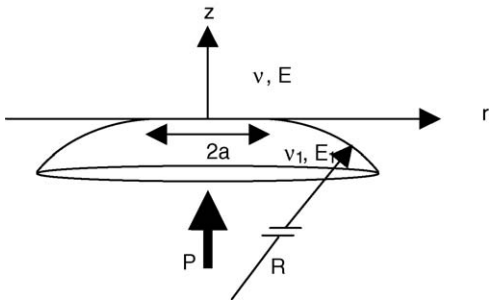

Fig. 2. Sketch of the ball-on-plate contact geometry.

made of spring steel and shot-peened at one side).[6] The most important shot peening parameters are indicated in the figures.

2.3. Determination of residual stresses and dislocation density

The residual stresses and dislocation densities were determined by X-ray diffraction (XRD). The full width at half maximum (FWHM) was determined to characterize the dislocation density. The macroscopic residual stresses were derived from the peak shift using the well known $\sin^2\psi$-method.[7] The most important measurement parameters are summarized in Table 2. The penetration depth from which 67% of the diffracted X-rays arise was in the range of 8–10 μm. For depth probing of residual stresses, it was necessary to remove stepwise thin surface layers by polishing using 3 μm diamond abrasives. This mechanical material removal resulted in additional small residual stresses.

2.4. Determination of static and cyclic load capacity

The static and cyclic load capacity was determined using the ball-on-plate test. The advantage of this test is the high surface sensitivity due to the rapidly decreasing tensile stresses with depth. The thickness of the tested surface layer is in the same range as the layer loaded in roller-bearings which are one of the target applications of shot peening. The tests were performed using an electro-mechanical and a servo-hydraulic testing machine. The load capacity was determined by stepwise increasing the load until cracks could be observed by optical microscopy. In case of the cyclic experiments 1,000,000 cycles with a frequency of 60 Hz were applied before inspection of the surface. At least five tests were performed per load step. A silicon nitride ball with a diameter of 10 mm was used for flat specimens; in case of bearing rollers a 4.76 mm ball had to be used to anticipate a failure of the indenter-ball.

2.5. Rolling test

The rolling tests were carried out with a testing device using the so-called "Amsler" configuration. Two discoidal silicon nitride specimens with a diameter of 39 mm are in rolling contact with controlled slip and load. One specimen has a cylindrical and the other a convex geometry in the raceway. This allows a high contact pressure without any edge effect. The tests were preformed under dry condition with 1% slip between the two rolling samples. Thus, compared to the ball-on-plate test, an additional sliding component was present. Beginning with 0.8 GPa, the contact pressure was stepwise increased every 5000 cycles until failure in the cylindrical sample could be detected by optical microscopy.

3. Stress state of the ball-on-plate contact

The stress field in the ball-on-plate contact can be calculated analytically in closed form.[8] Fig. 2 illustrates the

Table 1
Materials investigated and most important material characteristics

Material	Type manufacturer	Four-point bending strength (MPa)	Fracture toughness (MPa $m^{1/2}$)
Alumina[3]	A61 Kennametal Hertel	400	4.0
Silicon nitride[4]	N3208 C. Starck Ceramics	877	4.2
Silicon nitride[5]	XN8110 H.C. Starck Ceramics	860	6.2

Table 2
Parameters of residual stress evaluations by XRD

Material	Radiation	Lattice plane	X-ray elastic constant 1/2 s_2 (GPa^{-1})
Alumina	Cr Kα	{2 2 0}	3.15
Silicon nitride	Cr Kα	{4 1 1}	3.89

Table 3
Calculation of the maximum radial contact stress in the ball-on-plate contact[8]

$$\sigma_{rr,max} = \frac{(1-2\nu)p_0}{3}$$

$$p_0 = \frac{3P}{2\pi a^2}, \qquad a = \left(\frac{3RP}{4E^*}\right), \qquad \frac{1}{E^*} = \frac{(1-\nu^2)}{E} + \frac{(1-\nu_1^2)}{E_1}$$

$$-\frac{\sigma_{rr}}{p_0} = \left(\frac{1-2\nu}{3}\frac{a^2}{r^2}\left[1-\left(\frac{z}{\sqrt{u}}\right)^3\right] + \left(\frac{z}{\sqrt{u}}\right)^3 \frac{a^2 u}{u^2+a^2z^2} + \frac{z}{\sqrt{u}}\left[\frac{(1-\nu)u}{a^2+u} + (1+u)\frac{\sqrt{u}}{a}\arctan\frac{a}{\sqrt{u}} - 2\right]\right)$$

with

$$u = -\frac{a^2-z^2-r^2}{2} + \sqrt{\left(\frac{a^2-z^2-r^2}{2}\right) + z^2a^2}$$

geometrical loading situation and Table 3 gives the equations for the elastic radial contact stress. The required parameters are the elastic constants of the sphere and the plate (Young's modulus E, E_1; Poisson's ratio ν, ν_1), the ball radius R and the force P.

The tensile stress σ_{rr} is a function of r and z. Fig. 3 shows the stress field in a plate made of silicon nitride ($E = 300$ GPa, $\nu = 0.28$) when a 10 mm silicon nitride indenter ball is pressed with 4000 N on to the plate. Below the contact zone (width $a = 0.45$ mm) a compressive stress field exists. Near the surface outside the contact zone high tensile stresses are present. The maximum tensile stress $\sigma_{rr,max}$ occurs at the immediate surface near the boarder to the contact zone and it is linearly dependent on the Hertzian pressure p_0. In this example the highest tensile stress amounts 1373 MPa. The tensile stress field shows a strong gradient within the first micrometers of the near-surface layer. The 800 MPa contour line extends up to 6 μm into depth and the 400 MPa contour line up to 22 μm.

4. Results

4.1. Residual stress and static load capacity

The relationship between near-surface residual stresses and static load capacity was evaluated in detail for silicon nitride (N3208) and alumina. Fig. 4 correlates the near-surface stress states and the load capacities of polished and differently shot peened alumina and silicon nitride samples.

Shot peening allowed creating up to 1.3 GPa compressive residual stresses near the surface. These compressive stresses shifted the load needed to introduce a Hertzian cone-crack into the surface by a factor of 3 (silicon nitride) and 9 (alumina), respectively. The increase of near-surface strength was so high, that the load limit of the ball-on-plate testing device (11.7 kN) was reached in some cases and the samples passed the test without any crack. Thus, for the most effective shot peening process no error bar could be calculated for the fracture load.

The depth effect of the shot peening process was evaluated through depth probing of residual stresses and width of the diffraction lines (FWHM, a measure for the dislocation density) for silicon nitride N3208 and alumina. Fig. 5 shows that a lower peening pressure (0.2 MPa) results in the maximum compressive stress at the immediate surface whereas a higher peening pressure (0.3 MPa) results in maximum compressive residual stresses up to 2.0 GPa 25–30 μm below the surface. The peening process may affect an up to 80 μm thick near-surface.

The depth distributions of the diffraction line width (measure for dislocation densities), see Fig. 6, and macroscopic residual stresses are similar in shape. This indicates that the main driving force for the creation of compressive residual stress is micro-plastic deformation within the crystallites.

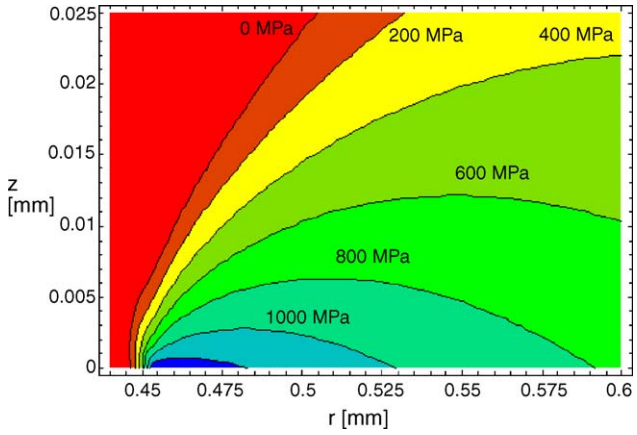

Fig. 3. Calculated stress fields in the plate for a 10 mm indenter ball which is pressed with 4000 N into the plate.

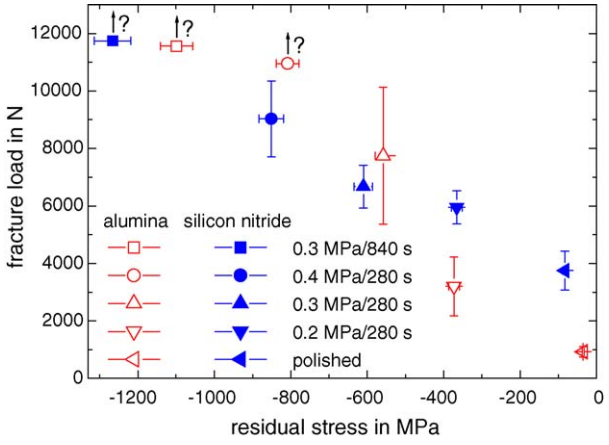

Fig. 4. Fracture load vs. residual stress of silicon nitride (N3208) and alumina samples in polished and different shot peened condition.

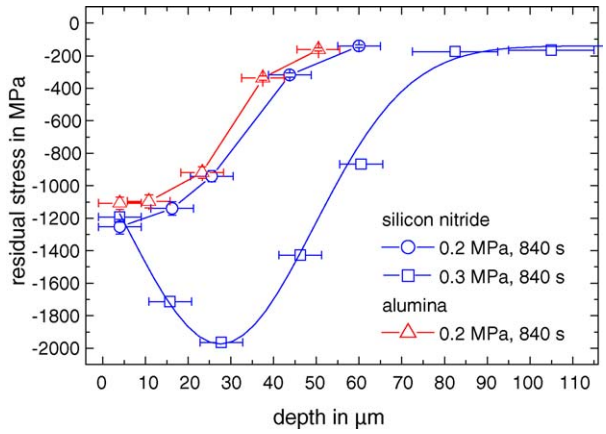

Fig. 5. Depth distribution of residual stresses of differently shot peened silicon nitride (N3208) and alumina samples.

4.2. Vickers indentation

The effect of high compressive residual stresses can easily be visualized by Vickers indentations. Figs. 7 and 8 compare indentations in polished and shot peened silicon nitride samples. The indentation was performed with a load of 10 N. The shot peened sample (0.3 MPa, 840 s) had been polished after shot peening to guaranty a surface roughness comparable to the polished reference sample (a few micrometers were removed using a 3 µm diamond abrasive). The reference sample developed the typical crack formation at the edges of the indentation (Fig. 7), whereas in the surface of the shot peened sample only very small cracks can be detected (Fig. 8).

4.3. Topography

During shot peening each hit of a bead will produce a localized deformation. The super-position of many localized deformations will result in an overall roughness of the surface. Fig. 9 shows a typical topography resulting from a shot peening process and Fig. 10 compiles the average roughness

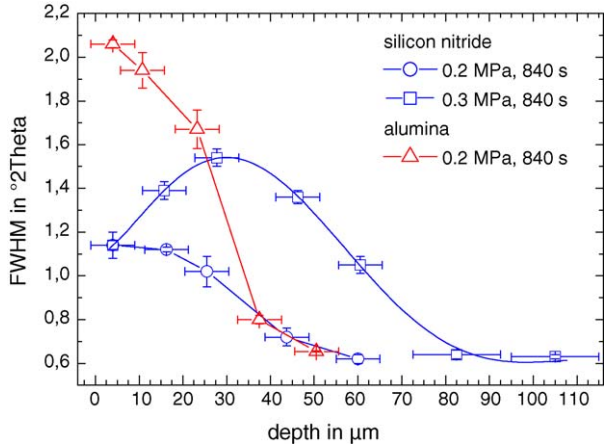

Fig. 6. Depth distribution of the width of the diffraction lines of differently shot peened silicon nitride (N3208) and alumina samples.

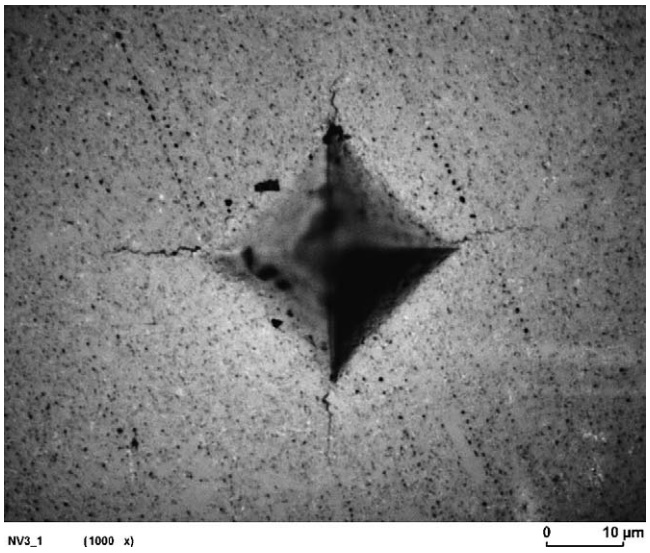

Fig. 7. Vickers indentation (9.81 N) in a polished silicon nitride sample.

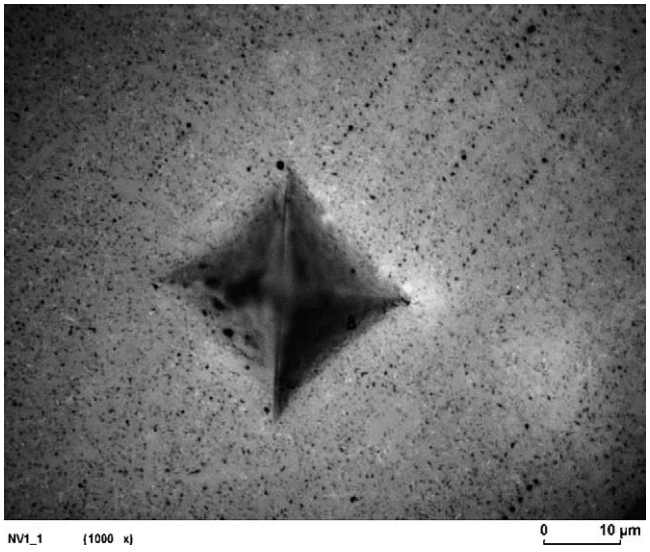

Fig. 8. Vickers indentation (9.81 N) in a shot peened (0.3 MPa pressure) silicon nitride sample. The sample was slightly repolished after shot peening to better show indentation-induced cracks.

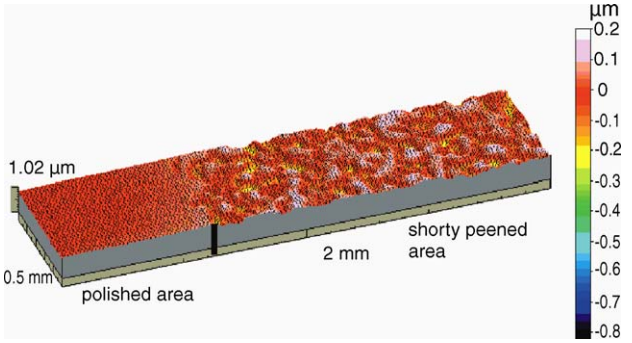

Fig. 9. Topographical map comparing a polished and a shot peened (0.2 MPa) silicon nitride surface area.

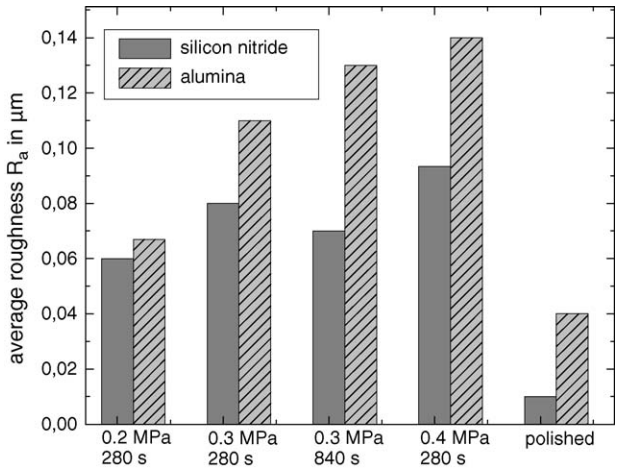

Fig. 10. Average roughness Ra of polished and shot peened silicon nitride (N3208) and alumina samples.

values of the alumina and silicon nitride surfaces in polished and different shot peened conditions.

The shot peening of the polished surface leads to a significant increase of the roughness. Nevertheless, the roughness of shot peened surfaces is comparable to surfaces in ground or lapped condition.

4.4. Static and cyclic load capacity

The influence of shot peening on the cyclic load capacity was determined in detail for silicon nitride N3208 using cyclic ball-on-plate tests. Fig. 11 shows the fracture probability as a function of the load for the shot peened and the polished reference surfaces. The given fracture probabilities are derived directly from the proportion of tests showing cracking.

For a fracture probability of 50%, the polished reference samples achieved a static load capacity of about 4 kN and a

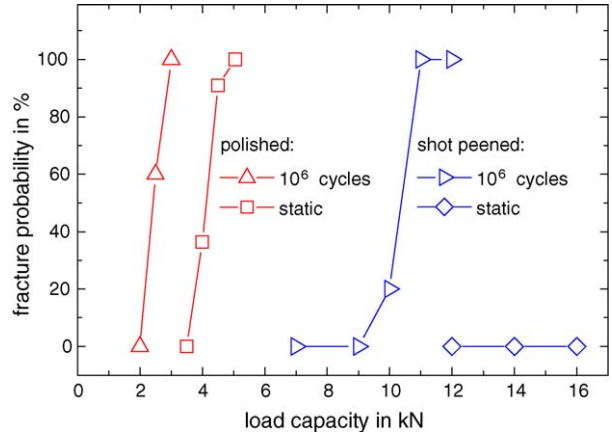

Fig. 11. Fracture probability of polished and shot peened samples (N3208), respectively, determined in static and cyclic ball-on-plate tests. Note that in case of the static tests of the shot peened samples the capacity of the test equipment was exceeded.

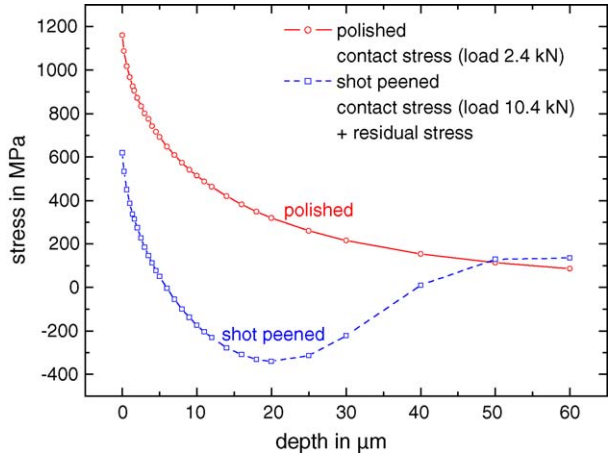

Fig. 12. Near-surface net fracture stress distribution of polished and shot peened silicon nitride samples.

cyclic load capacity of 2.4 kN. The cyclic load capacity of the shot peened samples reached 10.4 kN which is a gain of a factor of 4. The shot peening treatment increased the static load capacity to more than 16 kN. The capacity of the testing device was not high enough to introduce any cracks into the shot peened surface. From the result of no failure up to 16 kN a gain of the static load capacity of a factor of at least 5 can be concluded.

4.5. Analysis of net fracture stresses in the cyclic ball-on-plate tests

The net fracture stress in case of the shot peened condition is the sum of loading and residual stress. The net stresses were calculated for the polished and shot peened silicon nitride samples based on the experimentally determined fracture (50% fracture probability, Fig. 11) and the residual stress distribution (Fig. 5). The results are shown in Fig. 12. The maximum net stresses reach about 1.2 GPa at the surface of the polished samples (residual stresses due to polishing were neglected). This is significantly higher than the fracture strength of the bulk material (Table 1). The reason for this is the well known 'Weibull-behavior' of brittle materials which describes the increase of strength with decreasing volume due to the decreasing probability of fracture causing defects.

The fracture stress of brittle materials like silicon nitride is determined by the fracture toughness and the size, geometry and distribution of defects. Assuming only 'natural' defects in the material, comparable net stress fields should be evaluated for both near-surface conditions. This is obviously not fulfilled. The net fracture stress of the shot peened sample is lower compared to the fracture stress of the polished reference sample. Thus, it can be concluded that the used peening treatment also introduces some additional damage in the surface. Nevertheless, the increased cyclic load capacity of the shot peened specimens show that the peening induced residual stresses overcompensate the damage.

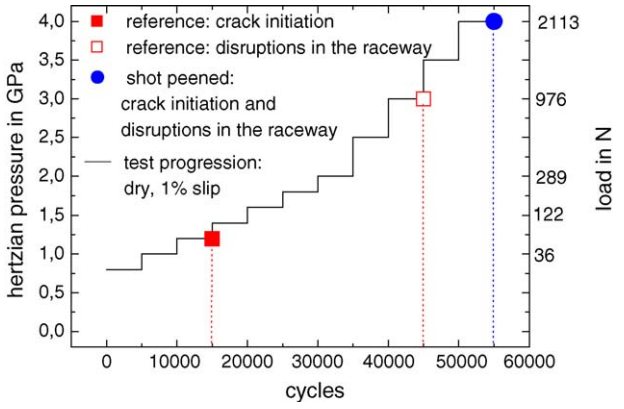

Fig. 13. Incremental rolling fatigue test on ground plus partially polished reference samples and additionally shot peened samples (N3208). The stepwise increase of load (and the corresponding Hertzian pressure) and the critical loads where crack initiation and severe damage was observed are indicated.

4.6. Rolling fatigue

Fig. 13 sketches the stepwise increase of the contact pressure during the experiment and indicates the critical load and number of cycles, where different stages of failure could be detected.

The first cracks in the raceway were observed in the polished reference sample after 15,000 cycles at a Hertzian pressure of 1.2 GPa (load = 62.5 N). In the shot peened samples, cracks appeared for the first time after 55,000 cycles at 4.0 GPa (load = 2113 N). Obviously, the shot peening treatment leads to an increase of the load capacity by a factor of 33 which corresponds to a three times higher applicable Hertzian pressure.

In spite of the early stage of damage in the reference samples the test was continued resulting in severe pitting and chipping after 45,000 cycles at a pressure of 3.0 GPa (load 976 N). Figs. 14 and 15 compares the damage patterns of the polished and the shot peened raceways, respectively, after totally 55,000 cycles applying up to 4.0 GPa pressure.

The comparison of severe damage in the raceway of the reference sample with numerous interacting cracks and large pitting areas and the only small sporadic cracks in the shot peened raceway illustrates the strengthening effect of the shot peening process.

4.7. Recovery of machining damage

The static load capacity of rollers (Ø 8 mm × 8 mm, XN8110) was determined before and after shot peening in rough-ground and finished surface condition, respectively. In contrast to all other ball-on-plate tests described in this paper, 4.76 mm diameter indenter-balls had to be used to anticipate a failure of the indenter-ball.

Comparing the load capacity of the finished and rough-ground rollers (see Fig. 16), a significant drop of strength is obtained due to machining damage introduced into the near-surface of the rough-ground rollers. Shot peening the rough-ground rollers not only compensates for the machining damage, but increases the load capacity above the level of the well-finished rollers. From the result that the load capacity is comparable to finished plus shot peened rollers, it can be concluded, that the shot peening process completely eliminated the influence of machining damage on the near-surface strength of the rollers.

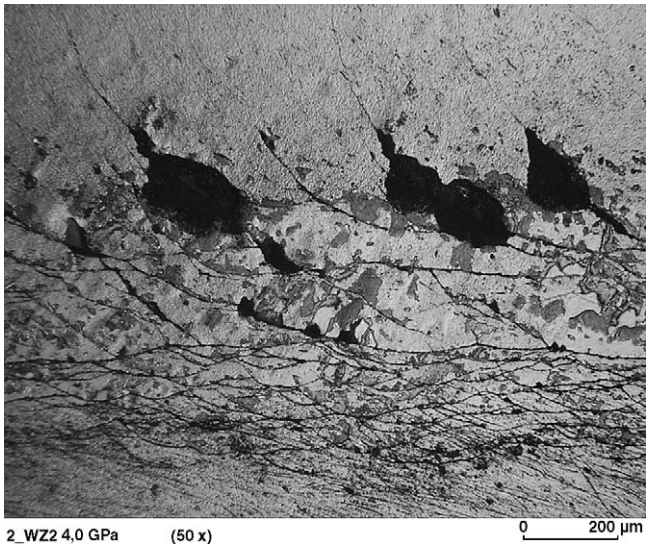

Fig. 14. Optical micrographs of a raceway after 55,000 cycles and a stepwise increase of the pressure up to 4.0 GPa. Interacting cracks and large-scale pitting in the polished sample.

4.8. Thermal stability

The high temperature stability of the shot peening induced residual stresses was evaluated for silicon nitride (N3208) by

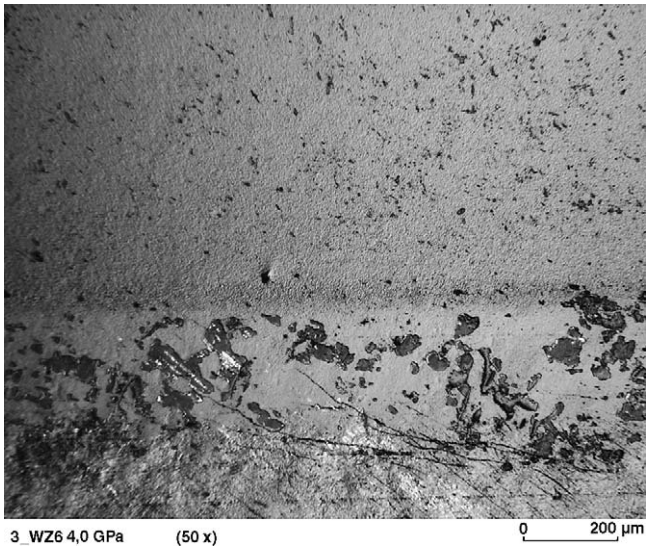

Fig. 15. Optical micrograph of a shot peened raceway after 55,000 cycles and a stepwise increase of the pressure up to 4.0 GPa. First small cracks are visible.

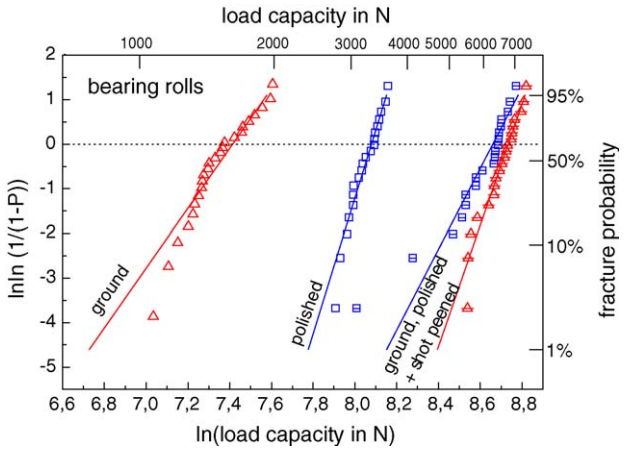

Fig. 16. Fracture probability of rollers (XN8110) in polished, ground and additionally shot peened condition, respectively (static ball indentation test performed on the cylindrical surfaces).

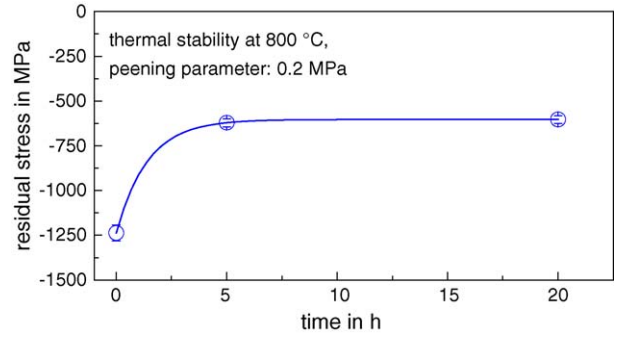

Fig. 17. Decline of shot peening induced residual stresses in silicon nitride N3208 at 800 °C.

XRD. Fig. 17 shows, that tempering samples at 800 °C leads to a 50% reduction of compressive residual surface stresses within the first 5 h. A further reduction could not be obtained within the next 15 h.

5. Conclusions

The presented investigations show that, using a novel shot peening process for brittle materials, micro-plastic deformation and high compressive residual stresses up to 2 GPa can be introduced into the near-surface of ceramics, declining within the first 100 μm. Tempering experiments, performed at 800 °C on silicon nitride revealed a satisfying stability of the shot peening effect. The shot peening process can dramatically increase the near-surface strength of ceramics. The static and cyclic load capacity tests show an increase of the load capacity by a factor 4, at least. The investigations performed on roller-bearing components in different surface conditions show that also roughly machined surfaces, which suffer from machining damage, can be improved dramatically by the shot peening process. Further investigations will concentrate on increasing the depth of the compressive residual stress field, on the effect of the residual stresses on the bending strength of ceramics and on the application of this promising technique to other types of ceramics.

Acknowledgements

Part of the investigations were supported by the Deutsche Forschungsge-meinschaft (DFG) under Grant No. Pf 314/3-2 and by the Bundesministerium für Forschung und Bildung (BMBF) under Grant No. 03N3075.

References

1. Pfeiffer, W. and Frey, T., Strengthening of ceramics by shot peening. *Mater. Sci. For.*, 2002, **404–407**, 101–108.
2. Pfeiffer, W. and Frey, T., Shot peening of ceramics: damage or benefit? *Ceramic Forum International* Cfi/Ber. DkG, 79 No. 4, E25, 2002.
3. Op de Hipt, M., Randzonencharakterisierung hartbearbeiteter und tribologisch belasteter Al_2O_3 und SiC-Keramiken. Fortschritt-Berichte VDI Reihe 5 Nr. 521, VDI-Verlag, 1998.
4. Rombach, M., *Experimentelle Untersuchungen und bruchmechanische Modellierung zum Versagensverhalten einer Siliciumnitridkeramik unter Kontaktbeanspruchungen*. PhD thesis, University Karlsruhe, 1995.
5. Data sheet H. C., *Starck Ceramics*.
6. Champaigne, J., *The Almen Gage and Almen Strip*. TSP, *Vol 4*, Issue 1, Spring 1990.
7. Müller, P. and Macherauch, E., Das $\sin^2\psi$-Verfahren der röntgenographischen Spannungsmessung. *Z. ang. Phys.*, 1961, **13**, 305–312.
8. Huber, M. T., Zur Theorie der Berührung fester elastischer Körper. *Annal. D. Physik B.*, 1904, **14**, 153–163.